POLISH MARITIME RESEARCH Special Issue 2017 S3 (95) 2017 Vol. 24; pp. 136-142
10.1515/pomr-2017-0116

MODELING AND ANALYSIS OF 12-PULSE INVERTER IN SHIPBOARD OR AIRCRAFT

Yanbo Che*
Jinhuan Zhou
Guojian Liu
Jianmei Xu
Yuancheng Zhao
Key Laboratory of Smart Grid of Ministry of Education, Tianjin University, China
* corresponding author

ABSTRACT

With the development of DC distribution system within the isolated power system of a ship or an aircraft, more constant frequency loads will be supplied by inverters connected to DC main bus. In the operating mode conversion process of an isolated power system, inverters will inevitably suffer from serious disturbance and affect the stability of the system. Therefore, it is important to establish a model of the inverter that reflects its dynamic characteristics and based on which to conduct the stability analysis. This paper proposes a 12-pulse inverter model based on the generalized state space averaging (GSSA) method. This model can overcome the limitations of 12-pulse inverter state space averaging (SSA) model in transient analysis with good accuracy and fast analysis ability effectively. Three kinds of models for a 12-pulse aircraft inverter are built in MATLAB, namely GSSA model, SSA model and detail device model. The simulation results show the high accuracy of GSSA model in stability analysis. This study provides an effective analytical tool for stability analysis of 12-pulse inverter and also provides a reference for inverter modeling research of isolated power system such as in aircraft or ship.

Keywords:

INTRODUCTION

With the concern of energy crisis and environment pollution, the application of electricity expands to various domains for its efficiency, cleanness and high quality energy [1]. The power supply in vehicles such as ship, aircraft and spacecraft is gradually replaced by electricity [2-4]. Isolated power system is characterized with localized power production and consumption, avoiding long distance transmission of electricity and supporting the costume-made according to the user demand. These characteristics make isolated power system well suited to new forms of power demand. Isolated power system such as ship, aircraft and spacecraft requires a multitude of power electronic converters during the process of power storage, transmission and consumption[5,6]. But the space is so limited that the proportion of power electronic device in isolated power systems is much larger than that in traditional interconnected electric power system.

Stimulated by the advantages of lightweight and energy saving, new vehicle isolated power system mostly adopts a distribution system based on DC main bus [7, 8]. The original AC loads in the AC power distribution system will be supplied by inverters connected to the DC main bus, which increase loads of inverters greatly. The stability of inverters will directly affect the safe and stable operation of the isolated power system [9-12].

So far, stability analysis of inverter largely depends on detailed device model and mathematical analytic model.

A power system model is employed in [13] to simulate the transient process of shipboard power system. The hardware in the loop simulation verification of the multiple inverters in aircraft power systems is performed in [14]. The device model is complicated in modeling, as it describes the thorough dynamic process of the system. On the other hand, it can't reveal the relationship between system parameters and system stability, which can't be used in system design and optimization. The mathematical analytic model is used to seek the analytic expression of the characteristics of the inverter by theoretical analysis, which can represent the steady-state and dynamic mathematical characteristics of the system. The most representative one is the state space averaging method. Being one of the most representative approaches, state space averaging method was applied to establish small-signal models of inverter for single-phase and three-phase [15, 16]. It was also used to build the state space averaging model of electromechanical actuators and rotating rectifier [17, 18]. However, in the derivation the state variables are assumed to have small change within the switching cycle and the dynamic characteristics of inverter are ignored, the state space averaging method cannot meet the fast response and dynamic analysis of large disturbance.

In 1991, Professor Seth R. Sanders and his students proposed the generalized state space averaging (GSSA) model, which is a tradeoff between the detailed device model and the simplified state space model [19]. Considering the invariant components of the state space model, GSSA also takes into account of the higher order components, which can be used not only for small disturbance analysis, but also for large disturbance analysis.

Taking into account of the electrical characteristics of the DC power distribution system, this paper applies the generalized state space method to build a 12-pulse inverter model in MATLAB/Simulink. The stability analysis is carried out based on the model, and the validity of the model by simulation results.

GENERALIZED STATE SPACE AVERAGING METHOD

Generalized state space averaging method employs the Fourier series with time-dependent coefficients. The signals are divided into invariants and high-order variables, and the order of precision is chosen according to actual needs. A waveform $x(t)$ over the interval [t-T, T] can be approximated with a Fourier series representation of the form

$$x(\mathrm{t}) = \sum_{k=-n}^{n} \langle x \rangle_k (\mathrm{t})\, \mathrm{e}^{jk\omega t} \tag{1}$$

Where $\omega = 2\pi / t$ is the fundamental angular frequency. When there is just invariant, k = 0, it is state space average. The higher orders take into consideration, the higher accuracy the results obtained. When n is infinite, the deviation between generalized state space operation and the actual error is zero, but the computation is large at this time. Hence, n depends on the required degree of accuracy. $\langle x \rangle_k$ is k-th Fourier coefficients defined as

$$\langle x \rangle_k (\mathrm{t}) = \frac{1}{T} \int_{t-T}^{t} x(\mathrm{t}) e^{-jk\omega t} dt \tag{2}$$

So a signal in (1) can be calculated and given by

$$x(\mathrm{t}) = \langle x \rangle_0 + 2 \sum_{k=1}^{\infty} \left\{ \mathrm{Re} \langle x \rangle_k \cos(\mathrm{k}\,\omega\,\mathrm{t}) - \mathrm{Im} \langle x \rangle_k \sin(\mathrm{k}\,\omega\,\mathrm{t}) \right\} \tag{3}$$

Three basic characteristics of Fourier transform are normally required, which are expressed by

$$\langle x(\mathrm{t}) + \mathrm{y}(\mathrm{t}) \rangle_k = \langle x \rangle_k (\mathrm{t}) + \langle y \rangle_k (\mathrm{t}) \tag{4}$$

$$\langle x(\mathrm{t})\, \mathrm{y}(\mathrm{t}) \rangle_k = \sum_{i=-\infty}^{\infty} \langle x(\mathrm{t}) \rangle_{k-i} \langle y(\mathrm{t}) \rangle_i \tag{5}$$

$$\frac{d}{dt} \langle x(\mathrm{t}) \rangle_k = \left\langle \frac{dx(\mathrm{t})}{dt} \right\rangle_k - jk\omega \langle x(\mathrm{t}) \rangle_k \tag{6}$$

MODELING AND ANALYSIS OF INVERTER

THE INVERTER CIRCUIT IN POWER ELECTRONIC

A circuit of SPWM-controlled 12-pulse voltage source inverter in isolated power system is shown in Fingure 1.

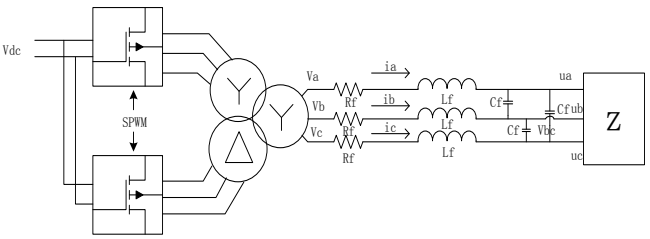

Fig. 1. 12-pulse voltage source inverter

The DC main bus voltage is shown by Vdc, which is 270V. Two three-phase inverters bridges, which connected through the Y-Δ/Y in parallel, are controlled by PWM. The transformer link was utilized to increase the voltage adjustment range. Since the neutral points of the AC load side and the DC main bus are not connected, line voltage measurement and analysis were adopted when building the generalized state space averaging model.

MODELING OF THE INVERTER CIRCUIT

The switching function s is defined as that s=1 means a switch is on, s=0 means off. The switch functions in a SPWM-controlled inverter, sui and sdi, $i \in \{a,b,c\}$, represent the states of up and down bridge arms in phase i, which satisfying $s_{ui} + s_{di} = 1$. The switching function is periodic, and can be replaced by Fourier series

$$s_1(t) = \sum_{n=1,\ \text{odd}}^{\infty} A_n \sin(n\omega t) \tag{7}$$

where An represents the coefficient of order n. The AC line voltage in the secondary side of the transformer can be expressed

$$v_{ab} = v_{ab1} + v_{ab2} \tag{8}$$

where v_{ab1} was generated by the first inverter bridge, and

$$v_{ab1}(\omega t) = v_{a1}(\omega t) - v_{b1}(\omega t) = \frac{m\sqrt{3}V_{dc}}{2n} \sum_{n=1,\ \text{odd}}^{\infty} A_n \sin[n(\omega t + \varphi + \frac{\pi}{6})] \tag{9}$$

where m is SPWM modulation ratio, n is the transformer ratio, An is n-th Fourier coefficient, φ is the initial phase angle. From symmetrical relationship we can obtain

$$\begin{cases} v_{bc1} = v_{ab1}(\omega t - 2\pi/3) \\ v_{ca} = v_{ab1}(\omega t + 2\pi/3) \\ v_{ab2} = v_{ab1}(\omega t + \pi/6) \\ v_{bc2} = v_{ab1}(\omega t - \pi/2) \\ v_{ca2} = v_{ab1}(\omega t + 5\pi/6) \end{cases} \tag{10}$$

where v_{ab2} , v_{bc2} and v_{ca2} are secondary side voltages of the transformer generated by the second inverter bridge.

Denote virtual line currents as i_{ab} , i_{bc} and i_{ca} . The three-phase loads are symmetrical, and their phase voltages or line currents are equal in amplitude with phase shift of 120°. According to the vector relation we can obtain

$$i_{ab} = \frac{1}{3}(i_a - i_b); i_{bc} = \frac{1}{3}(i_b - i_c); i_{ca} = \frac{1}{3}(i_c - i_a) \tag{11}$$

Suppose that the symmetrical loads are delta-connected with impedance Z_L , and AC side output currents and load voltages are selected as state variables, then

$$\begin{bmatrix} v_{ab} \\ v_{bc} \\ v_{ca} \end{bmatrix} = \begin{bmatrix} v_a - v_b \\ v_b - v_c \\ v_c - v_a \end{bmatrix} = \begin{bmatrix} L_f \frac{di_a}{dt} - L_f \frac{di_b}{dt} \\ L_f \frac{di_b}{dt} - L_f \frac{di_c}{dt} \\ L_f \frac{di_c}{dt} - L_f \frac{di_a}{dt} \end{bmatrix} + R_f \begin{bmatrix} i_a - i_b \\ i_b - i_c \\ i_c - i_a \end{bmatrix} + \begin{bmatrix} u_{ab} \\ u_{bc} \\ u_{ca} \end{bmatrix} \tag{12}$$

$$\begin{bmatrix} i_{ab} \\ i_{bc} \\ i_{ca} \end{bmatrix} = C_f \frac{d}{dt} \begin{bmatrix} u_{ab} \\ u_{bc} \\ u_{ca} \end{bmatrix} + \frac{1}{Z_L} \begin{bmatrix} u_{ab} \\ u_{bc} \\ u_{ca} \end{bmatrix} \tag{13}$$

where Rf, Lf and Cf are resistance, inductance and capacitance of low pass filter in Fig.1, respectively.

The state equation of inverter currents is constructed as

$$\frac{d}{dt}\begin{bmatrix} i_{ab} \\ i_{bc} \\ i_{ca} \end{bmatrix} = -\frac{R_f}{L_f}\begin{bmatrix} i_{ab} \\ i_{bc} \\ i_{ca} \end{bmatrix} - \frac{1}{3L_f}\begin{bmatrix} u_{ab} \\ u_{bc} \\ u_{ca} \end{bmatrix} + \frac{\sqrt{3}mV_{dc}}{6nL_f}\begin{bmatrix} \sin(\omega t + \varphi + \frac{\pi}{6}) + \sin(\omega t + \varphi + \frac{\pi}{3}) \\ \sin(\omega t + \varphi + \frac{5\pi}{6}) + \sin(\omega t + \varphi + \pi) \\ \sin(\omega t + \varphi - \frac{\pi}{2}) + \sin(\omega t + \varphi - \frac{\pi}{3}) \end{bmatrix} \tag{14}$$

$$\begin{bmatrix} i_{ab} \\ i_{bc} \\ i_{ca} \end{bmatrix} = C_f \frac{d}{dt} \begin{bmatrix} u_{ab} \\ u_{bc} \\ u_{ca} \end{bmatrix} + \frac{1}{Z_L} \begin{bmatrix} u_{ab} \\ u_{bc} \\ u_{ca} \end{bmatrix} \tag{15}$$

GENERALIZED STATE SPACE AVERAGING MODELING

Since the DC main bus bar contains few harmonic components, only the DC component is considered in the calculation. Combining with the generalized state space algorithms, the first order of the state variables is substituted into equation (12) and (14). The generalized state space variables are chosen as that, x_1 , x_2 ,... x_6 are DC components, x_7 , x_9 ... x_{17} and x_8 , x_{10} ... x_{18} are the real part and the imaginary parts of the fundamental component respectively, then the load-side voltages and AC currents can be expressed by

$$\begin{cases} \langle u_{ab} \rangle_0 = x_1, \langle u_{bc} \rangle_0 = x_2, \langle u_{ca} \rangle_0 = x_3; \\ \langle i_{ab} \rangle_0 = x_4, \langle i_{bc} \rangle_0 = x_5, \langle i_{ca} \rangle_0 = x_6; \\ \langle u_{ab} \rangle_1 = x_7 + jx_8, \langle u_{bc} \rangle_1 = x_9 + \mathrm{j}x_{10}, \\ \langle u_{ca} \rangle_1 = x_{11} + j\,x_{12}; \\ \langle i_{ab} \rangle_1 = x_{13} + \mathrm{j}x_{14}, \langle i_{bc} \rangle_1 = x_{15} + \mathrm{j}x_{16}, \\ \langle i_{ca} \rangle_1 = x_{17} + \mathrm{j}x_{18}; \end{cases} \tag{16}$$

Taking ZL=R and combining with the generalized state space algorithms, the final GSSA model is deduced as

$$\begin{bmatrix}\dot{x}_1\\ \dot{x}_2\\ \dot{x}_3\\ \dot{x}_4\\ \dot{x}_5\\ \dot{x}_6\end{bmatrix}=\begin{bmatrix}-\frac{1}{RC} & 0 & 0 & \frac{1}{C} & 0 & 0\\ 0 & -\frac{1}{RC} & 0 & 0 & \frac{1}{C} & 0\\ 0 & 0 & -\frac{1}{RC} & 0 & 0 & \frac{1}{C}\\ -\frac{1}{3L} & 0 & 0 & -\frac{R_f}{L_f} & 0 & 0\\ 0 & -\frac{1}{3L} & 0 & 0 & -\frac{R_f}{L_f} & 0\\ 0 & 0 & -\frac{1}{3L} & 0 & 0 & -\frac{R_f}{L_f}\end{bmatrix}\begin{bmatrix}x_1\\ x_2\\ x_3\\ x_4\\ x_5\\ x_6\end{bmatrix} \tag{17}$$

$$\begin{bmatrix}\dot{x}_7\\ \dot{x}_8\\ \dot{x}_9\\ \dot{x}_{10}\\ \dot{x}_{11}\\ \dot{x}_{12}\\ \dot{x}_{13}\\ \dot{x}_{14}\\ \dot{x}_{15}\\ \dot{x}_{16}\\ \dot{x}_{17}\\ \dot{x}_{18}\end{bmatrix}=\begin{bmatrix}-\frac{1}{RC} & \omega & 0 & 0 & 0 & 0 & \frac{1}{C} & 0 & 0 & 0 & 0 & 0\\ -\omega & -\frac{1}{RC} & 0 & 0 & 0 & 0 & 0 & \frac{1}{C} & 0 & 0 & 0 & 0\\ 0 & 0 & -\frac{1}{RC} & \omega & 0 & 0 & 0 & 0 & \frac{1}{C} & 0 & 0 & 0\\ 0 & 0 & -\omega & -\frac{1}{RC} & 0 & 0 & 0 & 0 & 0 & \frac{1}{C} & 0 & 0\\ 0 & 0 & 0 & 0 & -\frac{1}{RC} & \omega & 0 & 0 & 0 & 0 & \frac{1}{C} & 0\\ 0 & 0 & 0 & 0 & -\omega & -\frac{1}{RC} & 0 & 0 & 0 & 0 & 0 & \frac{1}{C}\\ -\frac{1}{3L} & 0 & 0 & 0 & 0 & 0 & -\frac{R_L}{L_f} & \omega & 0 & 0 & 0 & 0\\ 0 & -\frac{1}{3L} & 0 & 0 & 0 & 0 & -\omega & -\frac{R_L}{L_f} & 0 & 0 & 0 & 0\\ 0 & 0 & -\frac{1}{3L} & 0 & 0 & 0 & 0 & 0 & -\frac{R_L}{L_f} & \omega & 0 & 0\\ 0 & 0 & 0 & -\frac{1}{3L} & 0 & 0 & 0 & 0 & -\omega & -\frac{R_L}{L_f} & 0 & 0\\ 0 & 0 & 0 & 0 & -\frac{1}{3L} & 0 & 0 & 0 & 0 & 0 & -\frac{R_L}{L_f} & \omega\\ 0 & 0 & 0 & 0 & 0 & -\frac{1}{3L} & 0 & 0 & 0 & 0 & -\omega & -\frac{R_L}{L_f}\end{bmatrix}\begin{bmatrix}x_7\\ x_8\\ x_9\\ x_{10}\\ x_{11}\\ x_{12}\\ x_{13}\\ x_{14}\\ x_{15}\\ x_{16}\\ x_{17}\\ x_{18}\end{bmatrix}+$$

$$\frac{\sqrt{3}mV_{dc}}{12nR_f}\begin{bmatrix}0\\ 0\\ 0\\ 0\\ 0\\ 0\\ \sin(\varphi+\frac{\pi}{6})+\sin(\varphi+\frac{\pi}{3})\\ -\cos(\varphi+\frac{\pi}{6})-\cos(\varphi+\frac{\pi}{3})\\ \sin(\varphi-\frac{\pi}{2})+\sin(\varphi-\frac{\pi}{3})\\ -\cos(\varphi-\frac{\pi}{2})-\cos(\varphi-\frac{\pi}{3})\\ \sin(\varphi+\frac{5\pi}{6})+\sin(\varphi+\pi)\\ -\cos(\varphi+\frac{5\pi}{6})-\cos(\varphi+\pi)\end{bmatrix} \tag{18}$$

The load voltages and virtual line currents of inverter circuit can be expressed by generalized state variables as

$$\begin{cases}u_{ab}=x_1+2x_7\cos\omega t-2x_8\sin\omega t\\ u_{bc}=x_2+2x_9\cos\omega t-2x_{10}\sin\omega t\\ u_{ca}=x_3+2x_{11}\cos\omega t-2x_{12}\sin\omega t\\ i_{ab}=x_4+2x_{13}\cos\omega t-2x_{14}\sin\omega t\\ i_{bc}=x_5+2x_{15}\cos\omega t-2x_{16}\sin\omega t\\ i_{ca}=x_6+2x_{17}\cos\omega t-2x_{18}\sin\omega t\end{cases} \tag{19}$$

EXPERIMENTAL RESULTS

The circuit in Fig.1 is simulated to analyze the load line voltage Vab and the virtual line current Iab. Detail device model, SSA model and GSSA model are built in MATLAB/Simulink and their simulation results are compared and analyzed.

Parameters of 12-pulse inverter circuit are listed in the follow Table 1. SPWM is adopted in order to control the on-off states of the switches in inverters, and the equivalent resistance of three-phase symmetrical loads is 80Ω.

Tab. 1. The parameters of inverter circuit

Description	Symbol	Value	Unit
Main bus voltage	V_{dc}	270	V
Amplitude modulation ratio	m	0.8	—
Fundamental frequency	f	400	Hz
Switching frequency	f_{sw}	10800	Hz
Initial phase angle	φ	0	Rad/s
Filtering resistor	R_f	0.1	Ω
Filtering inductor	L_f	4.3	mH
Filtering capacitor	C_f	3.2	μF
Transformer ratio	n	2	—

Figure 2 (a) shows the block diagram of the detail device simulation of the 12-pulse inverter, and (b) is the GSSA model. The GSSA model reduces to SSA model when the state variables only contain zero-order part.

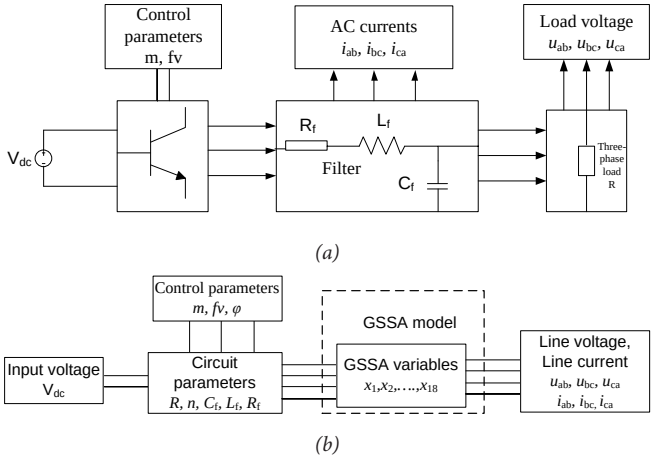

Fig. 2. Diagrams of the 12-pulse inverter
(a) simulation diagram of the detail device model
(b) simulation diagram of generalized state space averaging

Waveforms for SPWM signal and the transformer secondary voltage are shown in Figure 3.

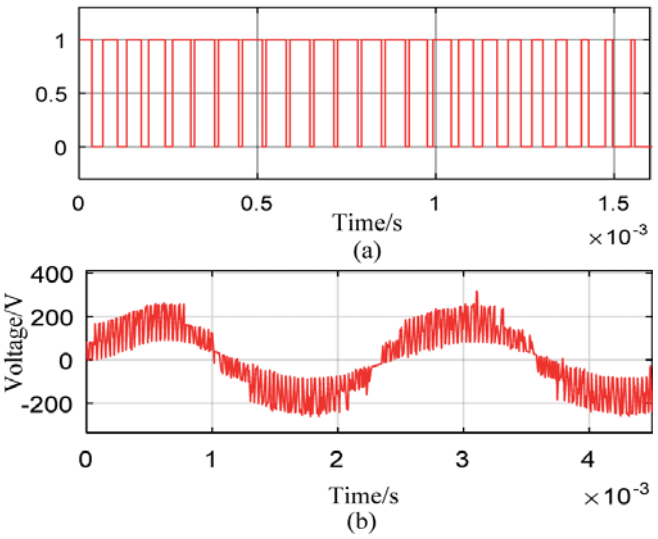

Fig. 3. SPWM modulation results
a) PWM signal output
(b) Transformer secondary voltage

Generated by the 12-pulse inverter and through the transformer, the secondary voltage waveform before low-pass filter contains a large number of high-order harmonics. Only when the parameters of the inverter circuit are appropriately set can the load gets qualified voltage.

When the power system switches its operating condition,the 12-pulse inverter is subject to large disturbance. Assuming that the inverter loads suddenly altered when the isolate power system changes its operation condition at 10ms, the load changes from 80Ω to 40Ω. The large signal disturbance will occur and affect the inverter.

The waveforms for the output line voltage Vab and the virtual current Iab are shown in Figure 4 and Figure 5. The results represent waveforms of detail device model, GSSA and SSA respectively.

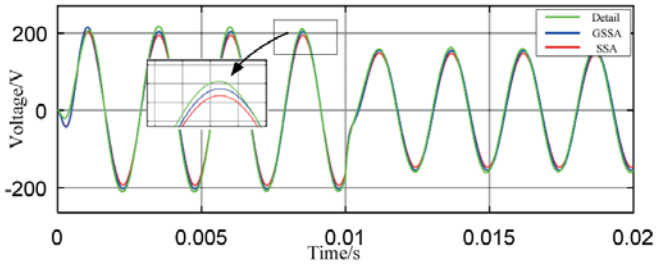

Fig. 4. Waveform of Vab voltage at load port

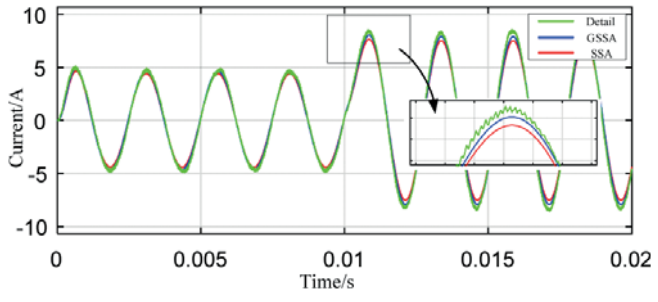

Fig. 5. Waveform of Iab at AC side

By comparing with the detail device simulation, the deviation of SSA model is about 6% when large signal disturbance occurred, and that of GSSA model is only about 3%. The accuracy of GSSA model is upgraded nearly doubled. Therefore, the results of GSSA model can better reflect the dynamic response process.

In addition, the voltage Vab and the current Iab of three models are analyzed with fast Fourier transform. The fundamental frequency is 400Hz. Contents of harmonics under 5th order are shown in Table 2 and Table 3.

Tab. 2. Comparison of current harmonic analysis of three models (unit:%)

Harmonic frequency	0	400	800	1200	1600	2000	Total harmonic
Switch	3.58	100	9.99	6.21	3.20	1.93	12.53
GSSA	3.26	95.8	9.01	5.68	2.93	1.77	12.04
SSA	2.55	87.7	7.15	4.33	2.14	1.55	9.25

Tab. 3. Comparison of voltage harmonic analysis of three models (unit:%)

Harmonic frequency	0 DC	400	800	1200	1600	2000	Total harmonic
Switch	3.88	100	18.39	11.96	8.63	6.79	27.67
GSSA	3.22	93.6	17.24	9.25	6.63	5.67	22.20
SSA	2.59	85.2	10.73	8.23	5.25	4.05	16.17

Figure 6 shows the comparison between the harmonic values of Vab and Iab when the inverter suffers large disturbance.

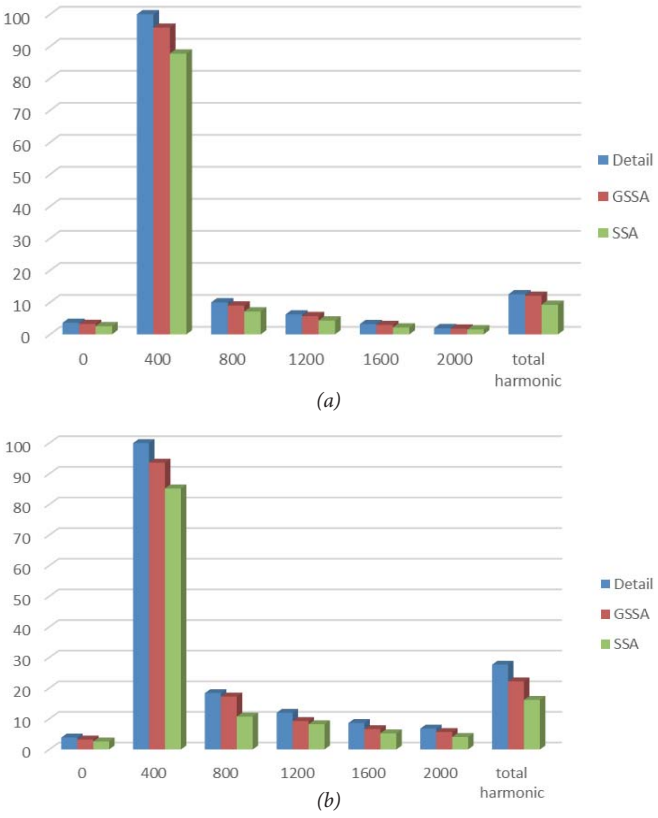

Fig. 6. The comparison of models
(a) current harmonic analysis of three models
(b) voltage harmonic analysis of three models

In consideration of high-order variables, the generalized state space model can analyze the harmonic content accurately when the power system encounters large disturbance. Compared with the SSA model, this model has a great improvement on the first-order harmonic analysis and increases the accuracy of the analysis of high-order harmonic content.

Simulation speeds for the three models are shown in Table 4.

Tab. 4. Experimental simulation speed

model	Simulation t(s)
Detail device model	60
State space averaging	10
Generalized state space averaging	13

Compared with the state space averaging model, the generalized state space averaging model spends more than 30% time, but its analysis accuracy has been greatly improved, can well meet the analysis requirements of 12-pulse inverter in the accuracy of stability analysis.

CONCLUSION

Based on the GSSA approach, a model of 12-pulse inverter commonly used in isolated power systems is built in the MATLAB simulation environment. The following conclusions can be drawn from the theoretical and experimental analysis:

(a) Compared with the state space modeling approach, GSSA modeling considers high order components. The higher the order is, the smaller the error will be. The error will have a tendency to zero when the order tends to infinity. Selection of order is determined by the required accuracy and simulation speed.

(b) The GSSA model containing high order components can reflect the actual dynamic characteristics of the inverter, and can improve the accuracy of harmonic analysis of the 12-pulse inverter under large disturbances like operation mode conversion. Having a perfect utilitarian value, this model can meet the requirements of isolated power system analysis including not only small disturbance stability but also large disturbance variation under working conditions switching.

Therefore, the GSSA model offers good feasibility and accuracy in analysis, can provide a basic model for the analysis of large-disturbance dynamic characteristics of 12-pulse inverter circuit. In addition, this model can also be applied to the analysis of other isolated power systems.

ACKNOWLEDGMENTS

This research was financially supported by National Natural Science Foundation of China (Grant No. U1533126).

REFERENCES

1. L. J. Chen, S. W. Mei, X. U. Yin, et al, 2011. A new pattern of future power grids:Isolated power system. *Journal of Electric Power Science & Technology.*
2. Y. Khersonsky, N. Hingorani, K. L. PetersSon, 2009. IEEE Electric Ship Technologies Initiative. I*EEE Industry Applications Magazine*, 17(1), 65-73.
3. M. Hirst, A. Mcloughlin, P. J. Norman, et al, 2011. Demonstrating the more electric engine: a step towards the power optimised aircraft. *Iet Electric Power Applications,* 5(1), 3-13.
4. L. T. Lam, R. Louey, 2006. Development of ultra-battery for hybrid-electric vehicle applications. *Journal of Power Sources,* 158(2), 1140-1148.
5. L. Prisse, D. Ferer, H. Foch, et al, 2009. New power centre and power electronics sharing in aircraft. European Conference on Power Electronics and Applications. IEEE .pp. 1-9.
6. K. P. Logan,2007. Intelligent diagnostic requirements of future all-electric ship integrated power system. *IEEE Transactions on Industry Applications,* 43(1), 139-149.
7. K. Satpathi, A. Ukil, N.Thukral, et al, 2016. Modelling of DC Shipboard Power System. IEEE International Conference on Power Electronics, drives and Energy Systems. IEEE.
8. Y. Wang, C. Xiang, S. Hu,2014. Design and control strategy for a new hybrid energy storage system. Applied Power Electronics Conference and Exposition. IEEE. 3401-3405.
9. D. Izquierdo, R. Azcona, F. J. L. Del Cerro, et al, 2010. Electrical power distribution system (HV270DC) for application in more electric aircraft. Applied Power Electronics Conference and Exposition (APEC). Palm Springs: IEEE. 1300-1305.
10. C. R. Avery, S. G. Burrow, P. H. Mellor, 2007. Electrical generation and distribution for the more electric aircraft. Universities Power Engineering Conference(UPEC) 2007. Brighton: IEEE. 1007-1012.
11. H. Zhang, F. Mollet, C. Saudemont, et al,2010. Experimental validation of energy storage system management strategies for a local dc distribution system of more electric aircraft. *Industrial Electronics,* 57(12), 3905-3916.
12. T. Wu, S. V. Bozhko, G. M. Asher, 2010. High speed modeling approach of aircraft Electronical power systems under both normal and abnormal scenarios. International Symposium Industrial Electronics (ISIE). Bari: IEEE. 870-877.

13. 15 Real-Time Distributed Coordination of Power Electronic Converters in a DC Shipboard Distribution System

14. S. R. Mathew, P. V. R. Sai Kiran,M. Anand, 2014. Design and implementation of a three level diode clamped inverter for more electric aircraft applications using hardware in the loop simulator. 2014International conference on Advances in Electronics, Computers and Computers Communications(ICAECC). Bangalore: IEEE. 1-6.

15. S. Ahmed, Z. Shen, P. Mattavelli, et al, 2011. Small-signal model of a Voltage Source Inverter (VSI) Considering the Dead-Time Effect and Space Vector Modulation Types. The 26th annual Applied Power Electronics Conference and Exposition. Fort worth: IEEE. 685-690.

16. D. Y. Hyun, C. S. Lim, R. Y. Kim, et al,2013. Averaged modeling and control of a single-phase grid-connected two-stage inverter for battery application. Industrial Electronic Society. Vienna: IEEE. 489-494.

17. T. Wu, S. Bozhko, G. M. Asher, et al,2008. Fast reduced functional models of electromechanical actuators for more-electric aircraft power system study. Bellevue WA: SAE Technical Paper.

18. T.Wu, S. V. Bozhko, G. Asher, et al,2009. A Fast Dynamic Phasor Model of Autotransformer Rectifier Unit for More Electric Aircraft. Industrial Electronics 35th Annual Conference of IEEE. Porto: IEEE. 2531-2536.

19. S. R. Sanders, J. M. Noworolski, X. Z. Liu, et al,1991. Generalized averaging method for power conversion circuits.*Power Electronics IEEE Transactions on*, 6(2), 251-259.

CONTACT WITH THE AUTHORS

Yanbo Che

Key Laboratory of Smart Grid of Ministry of Education,
Tianjin University
Tianjin 300072
China